EVOH/Clay Nanocomposites Produced by Dynamic Melt Mixing

N. ARTZI[1], M. NARKIS[1]*, *and* A. SIEGMANN[2]

[1]*Department of Chemical Engineering*
[2]*Department of Materials Engineering*
Technion – IIT, Haifa 32000, Israel

Ethylene-vinyl alcohol copolymer (EVOH)/clay nanocomposites were prepared via a dynamic melt-intercalation process using a Brabender Plastograph or extruder. The phase morphology and the crystallization behavior of the nanocomposites were investigated, using differential scanning calorimetry (DSC), X-ray diffraction (XRD), and transmission electron microscopy (TEM). Mechanical properties were determined using an Instron machine. It was found that the viscosity of EVOH/clay mixtures increases with processing time. Thermal analysis of the EVOH/clay nanocomposites showed that the melting temperature, crystallization temperature, and heat of fusion of the EVOH matrix sharply decrease when clay is added. XRD verified an increased gallery height for the clay in the composites. Maleic anhydride–grafted ethylene vinyl acetate (EVA-g-MA) or maleic anhydride–grafted linear low-density polyethylene (LLDPE-g-MA) were added as compatibilizers of EVOH with clay, in various concentrations (1, 5 and 10 wt%). Significantly higher viscosity levels were obtained for the compatibilized systems as the torque dramatically increased when processed in the Brabender machine. Enhanced intercalation within the galleries was obtained. EVOH crystallinity decreased with increasing compatibilizer content, until at a certain content no crystallization took place. EVOH/clay composites were also processed in an extruder, showing improved mechanical properties for as low as 1 wt% clay. The strong EVOH/clay interactions are responsible for the unique behavior of their nanocomposites. Polym. Eng. Sci. 44:1019–1026, 2004.

INTRODUCTION

Polymer melt intercalation is a promising new approach for fabricating polymer-layered silicate nanocomposites, apparently by using a conventional melt-mixing technology. The absence of solvents makes direct intercalation an environmentally sound and economically advantageous method (1). A strong interaction of the silicates with the polymer matrix, attained by compatibilization of the layered silicate with prudently chosen intercalants, leads to polymer melt penetration into the silicate galleries, i.e., to melt intercalation. As polymer-silicate interactions become stronger and intercalation progresses, the gallery height increases, and, under the dynamic process, exfoliation may take place. Intercalation, followed by delamination processes, leads to dispersion of nano-scale thick clay platelets. Such systems exhibit improved modulus and strength, practically without affecting the impact resistance, as is usually the case for conventional filled polymers. Also, quite often, the thermal stability, e.g., heat distortion temperature (HDT), increases. The dispersed clay platelets may strongly affect permeability by dictating a tortuous pathway for permeant molecules transversing through the nanocomposite. The combined enhanced barrier characteristics, chemical resistance, reduced solvent uptake and flame retardancy of clay-polymer nanocomposites all benefit from the hindered diffusion pathways through the nanocomposite.

It is generally accepted that exfoliated systems give better mechanical properties than intercalated ones (2). Generally, the degree of dispersion is governed by the matrix viscosity, average shear rate, and the mean residence time in the mixing process (3).

In recent years, numerous research works were reported in the field of clay-nanocomposites, using such polymers as nylon 6, polypropylene, and polystyrene as

*To whom correspondence should be addressed.
E-mail: narkis@tx.technion.ac.il

Published online in Wiley InterScience (www.interscience.wiley.com).
DOI: 10.1002/pen.20095

matrices, and DSC, XRD, TEM, and other methods for characterization (4–16). These studies have shown higher matrix melting temperatures (T_m), crystallization temperatures (T_c) and enthalpy values compared to the neat matrices, without any DSC evidence for the existence of a glass transition temperature (T_g). Compatibilization is a common method to mediate and increase interaction between phases, enhancing formation of the desired morphology and the associated mechanical properties. In general, compatibilizers reduce interfacial tension, hence increasing interphase adhesion, leading to a finely dispersed morphology and stability against gross segregation. This study focuses on the influence of compatibilizers, i.e., maleic anhydride–grafted EVA, EVA-g-MA, or maleic anhydride–grafted LLDPE, LLDPE-g-MA, and processing conditions on the resulting EVOH/clay nanocomposite morphology, intercalation/exfoliation levels, and the thermal and mechanical behavior. The EVOH/clay proportion, 85/15, was selected in most of the data presented here, similar to the previous works (17, 18), to magnify the phenomena observed. Much lower clay concentrations are currently studied, aiming at the development of useful physical properties of EVOH/clay nanocomposites.

EXPERIMENTAL

Materials

The EVOH (ethylene-vinyl alcohol copolymer) used in this study is a commercial product, Kuraray, Japan, consisting of 32 mole% ethylene. Two types of treated clay were used: 1) Nanomer-I.30E, an onium ion surface-modified montmorillonite mineral. The organoclay contains 70–75 wt% montmorillonite and 20–25 wt% octadecylamine. It is claimed to be designed for ease of dispersion into amine-cured epoxy resins to form nanocomposites; 2) Nanomer-I.35L, a surface-modified montmorillonite mineral treated for EVOH resin. Both were obtained from Nanocor, Illinois, USA. Two types of compatibilizers were studied: EVA-g-MA (maleic anhydride–grafted ethylene-vinyl acetate), tradenamed Orevac, from Atofina, France; and LLDPE-g-MA (maleic anhydride–grafted linear low-density polyethylene) from Mitsui, Japan. Both contain less than 2 wt% MA.

Preparation Methods

Prior to melt blending, the EVOH copolymer was milled into a powder. The polymer and clay powders were dried in a vacuum oven at 80°C and 60°C, respectively, for 15 hrs. The components were dry-blended at selected ratios, and subsequently melt-mixed at 230°C at 60 rpm, in a Brabender Plastograph, equipped with a 50 cm^3 cell at different mixing times (10 and 45 minutes). The melt-mixing step was also performed in a counter-rotating, intermeshing, twin-screw extruder, Brabender TSC 42/6 (L/D = 6; D = 42 mm). The components were melt-mixed at several temperatures (200°C and 220°C in all zones) and screw rotation speeds (20 and 40 rpm). Filaments of the various blends produced were ground and then injection molded using an Arburg 220/150 injection molding machine, equipped with an ASTM standard mold. The injection molding machine temperature was maintained at 200°C or 220°C in all zones, and the mold at 40°C.

Characterization

The phase morphology of the blends was studied by SEM and TEM. Differential scanning calorimetry (DSC) was employed for characterizing the thermal behavior of the composites. The layered structure of the clay was examined by XRD. Tensile properties of injection molded "dogbone" specimens were determined using an Instron machine.

RESULTS AND DISCUSSION

Intercalation and/or delamination of clay in the presence of EVOH can be accomplished by melt-mixing in a Brabender Plastograph. *Figure 1* shows the mixing torque as a function of mixing time for 85/15 EVOH/clay systems, for two types of clay, treated (1.30E) and untreated. Under the dynamic mixing conditions, the gradual viscosity increase reflects on the fracturing of the organoclay particles into small aggregates and also between lamina, followed by a delamination process, eventually leading to blending of thin platelets into the EVOH matrix. Under static "blending" conditions, i.e., prolonged heating without shearing, intercalation is the dominant step (19–21). However, under dynamic conditions, delamination, in addition to intercalation, may be a major step, with a suggested onion-like delamination characteristic behavior for highly interacting clay/matrix systems. *Figure 1* shows that the viscosity

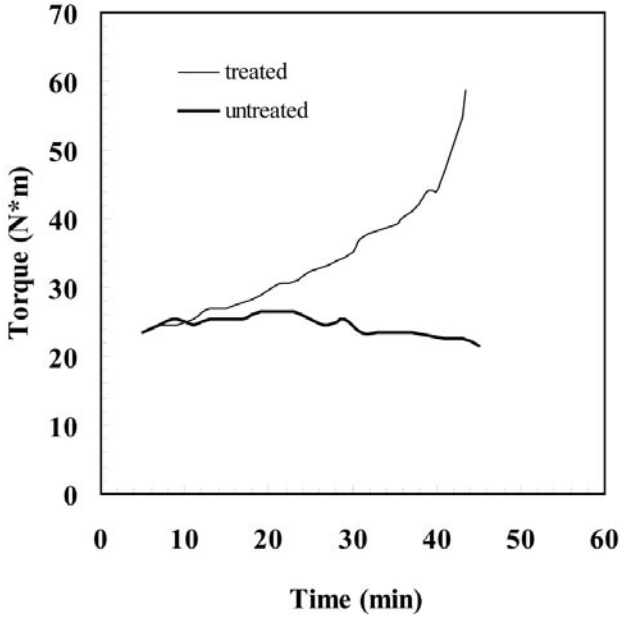

Fig. 1. Brabender plastograms of 85/15 EVOH/I.30E clay blends at 230°C and 60 rpm.

of the composite with the untreated clay is almost constant, implying that the clay particles stay practically intact, behaving as regular filler particles. However, the viscosity of the system with treated clay rises because of fracturing processes, formation of new surfaces, and additional interaction with the EVOH matrix. When a continuous-platelet network is established, flow mechanisms such as plug flow, slip at the wall phenomena, and even mechanical fracturing of the hot mass in the mixing cell are taking place (22).

Figure 2 depicts X-ray diffraction patterns for the neat EVOH, treated clay, and the composites of 85/15 EVOH/treated clay, which were processed for 10 and 45 min at 230°C. The basal reflections, characteristic of the virgin treated clay ($2\theta = 3.58°, 8.12°$; $d_{(001)} = 2.46$ nm) and the neat polymer ($2\theta = 10.78°, 20.1°, 21.24°$), are included in the diffraction pattern. As a result of the melt-mixing process, for the EVOH/treated clay system, the characteristic peaks of the treated clay shift to lower degrees ($2\theta = 2.7°, 5.5°, 8.34°$; $d_{(001)} = 3.26$ nm) and ($2\theta = 2.72°, 5.42°, 8.12°$; $d_{(001)} = 3.25$ nm) for 10 and 45 min, respectively, which is attributed to intercalation. That is, a 10-min processing duration is a sufficient time for intercalation to occur. Further mixing may thus lead to a better dispersion of the already intercalated clay.

Figure 3 shows TEM images of EVOH containing 5 and 15 wt% clay of both types, I.30E and I.35L-clay. The light gray area is the EVOH matrix and the darker regions are made up of the silicate layers. Both intercalated and delaminated regions can be seen. The intercalated regions (*Figs. 3a, c, d*) have a microstructure similar to that of the treated clay (periodical ordered structure), but the interlayer distance is expanded to 3–4 nm, which is compatible with the XRD results. However, some of the silicate layers were exfoliated into nanometer layers and randomly dispersed in the polymer matrix via the dynamic melt-mixing (*Figs. 3a, b, c*). The blends exhibit mixed morphology, i.e., intercalated and delaminated. The exfoliated structure is more evident at the lower clay content for both clay types (*Figs. 3a, b* compared to *Figs. 3c, d*), as expected. However, the blend containing 5 wt% L-clay (*Fig. 3b*) shows regions of fully exfoliated structure.

EVOH/clay composites were also processed in an extruder. The residence time in the extruder was several minutes; therefore, the torque is constant with mixing time. However, the blends' torque level is significantly higher than that of neat EVOH in most of the blending conditions used. Moreover, the torque level has reached the allowed force limit; therefore the highest clay content used was 1 wt%. Higher loadings could cause severe damage to the machine. In order to explore the effect of residence time on the composites formed, the composites were reinserted into the extruder for three successive passes. Even after the first pass, the torque was very high, implying that clay particles were still being exfoliated.

The X-ray diffraction patterns of EVOH containing 0.5 wt% 1.35L clay processed at 200°C and 40 rpm do not show a characteristic basal reflection (*Fig. 4*), which is indicative of an exfoliated structure. Owing to the high interaction level between the polar EVOH and the treated clay, under high levels of shear stress in

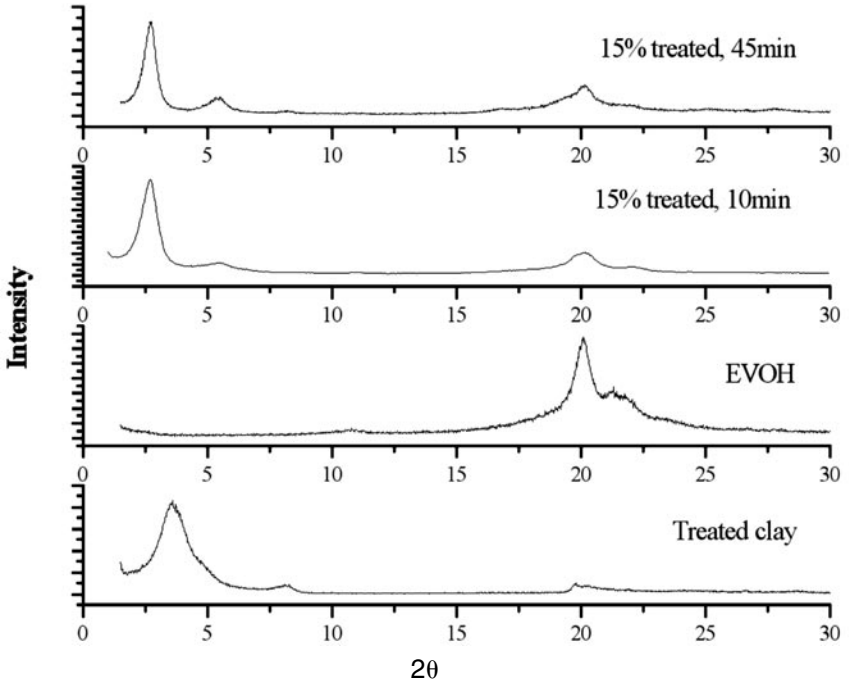

Fig. 2. X-ray diffraction patterns of neat I.30E clay, neat EVOH and 85/15 EVOH/I.30E clay blend, prepared by 10 and 45 min of mixing in the Brabender cell, at 230°C.

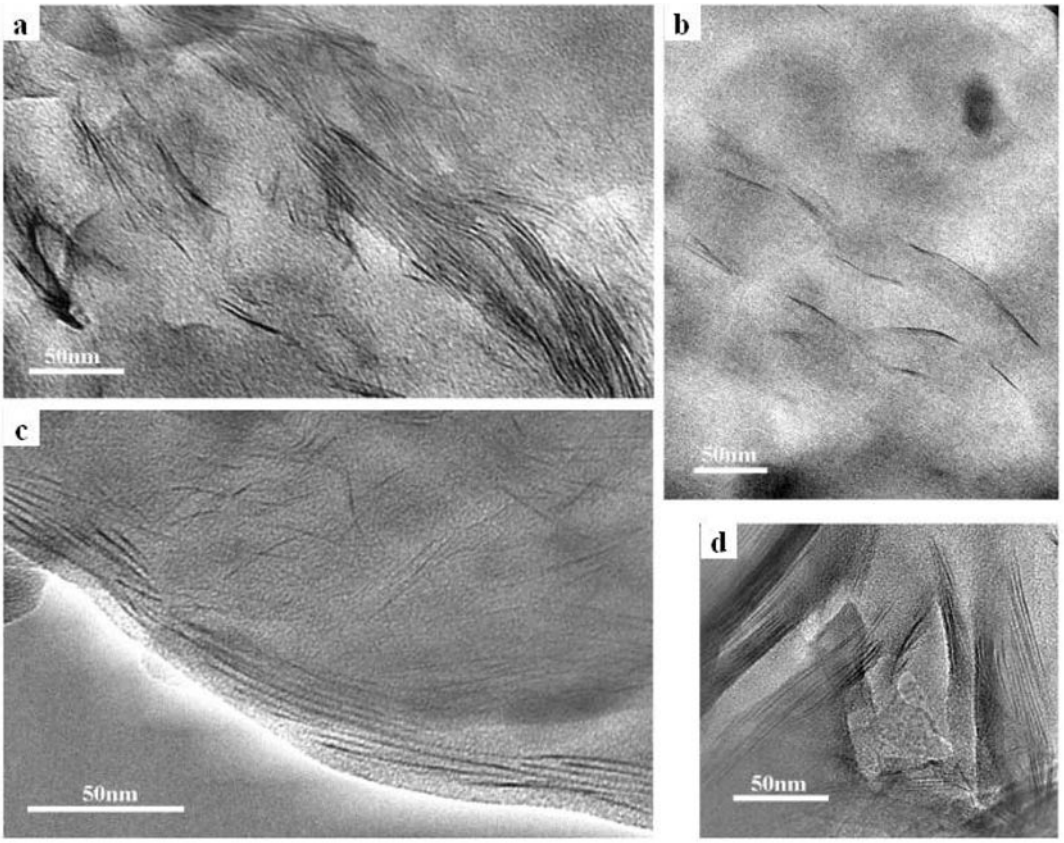

Fig. 3. TEM micrographs of EVOH blends prepared by mixing in the Brabender cell, at 230°C (bar = 50 nm): (a) [95/5 EVOH/I.35L clay], (b) [95/5 EVOH/I.30E clay], (c) [85/15 EVOH/I.30E clay], (d) [85/15 EVOH/I.35L clay].

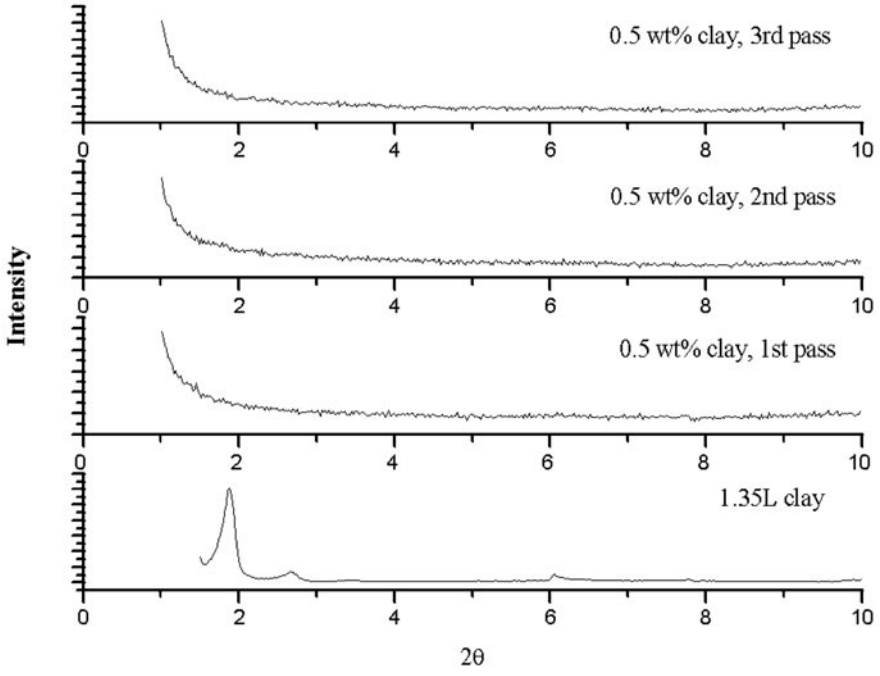

Fig. 4. X-ray diffraction patterns of neat I.35L clay, and EVOH containing 0.5 wt% clay after three successive passes in the extruder at 200°C and 40 rpm and injection molding.

the extruder, dispersion of individual platelets can be achieved. A typical stress-strain diagram for EVOH and clay processed at 200°C is shown in *Fig. 5*. At a processing temperature of 200°C, regardless of clay type or content, the strength and modulus were substantially increased relative to neat EVOH without significant variation in toughness or impact strength as measured by the standard Izod test. Modulus and yield strength improvement upon the addition of only 0.5 wt% 1.35L clay reached 40% and 30%, respectively, which is significant for that low clay content.

In summary, in highly interacting systems, in addition to a fracturing process of the clay particles, an onion-like delamination process is suggested, as schematically illustrated in *Fig. 6*. External platelets are subjected to dynamic high shear forces, which ultimately cause their delamination from the stack of layers building the original clay particle. Depending on the processing conditions and clay content, the morphology obtained can be mixed intercalation and exfoliation or complete exfoliation.

In an attempt to further improve the interaction level between the EVOH matrix and the clay tactoids, and simultaneously increase the level of intercalation and exfoliation, different compatibilizers were added, i.e., EVA-g-MA and LLDPE-g-MA (23). *Figure 7* shows the mixing torque as a function of mixing time for the systems containing EVA-g-MA as a compatibilizer. The plastograms are affected by the EVA-g-MA content and show an abrupt torque upturn. The viscosity of EVA-g-MA containing 15 wt% clay (without EVOH) is low and decreases slightly with time. However, adding 5 and 10 wt% EVA-g-MA to the EVOH/clay system shortens the time for the torque to rise. The neat EVOH, neat EVA-g-MA, and blends containing the same amounts of EVA-g-MA (without clay, not shown here) show a stable constant torque as a function of mixing time. The sharp torque decrease seen after 40 min of mixing when 10 wt% compatibilizer was incorporated, in the presence of 15 wt% clay, is a result of mechanical grinding into powder of the hot mass under the dynamic mixing conditions. The viscosity of LLDPE-g-MA containing 15 wt% clay is also low and decreases with time, as for EVA-g-MA (not shown here). The same trend of torque upturn is noticed after shorter times by comparison with the reference 85/15 EVOH/clay blend. However, the torque decrease is seen already for the 5 wt% compatibilizer (compared to 10 wt% in the former case). The blends containing different amounts of compatibilizer based on LLDPE in the absence of clay (not shown here), showed constant torque values with time, similar to the EVA-g-MA compatibilizer systems. Although LLDPE-g-MA viscosity is similar to that of neat EVOH and therefore higher than that of EVA-g-MA, the blends containing the same amounts of compatibilizers exhibited lower torque values when LLDPE-g-MA was used. Overall, the gradual viscosity increase, which is more pronounced in the presence of the compatibilizers, is indicative of more fracturing of the clay particles.

Figure 8 shows the X-ray diffraction pattern of neat clay, 85/15 EVOH/clay, and blends containing EVA-g-MA as compatibilizers. The increase in the clay basal spacing in the presence of EVOH is higher for the compatibilized systems, and is more significant for larger compatibilizer amounts. The neat clay shows a characteristic peak at $2\theta = 3.58°$ ($d_{001} = 25Å$). The incorporation of 15 wt% clay into EVOH has resulted in an intercalated structure with a gallery spacing of 32Å

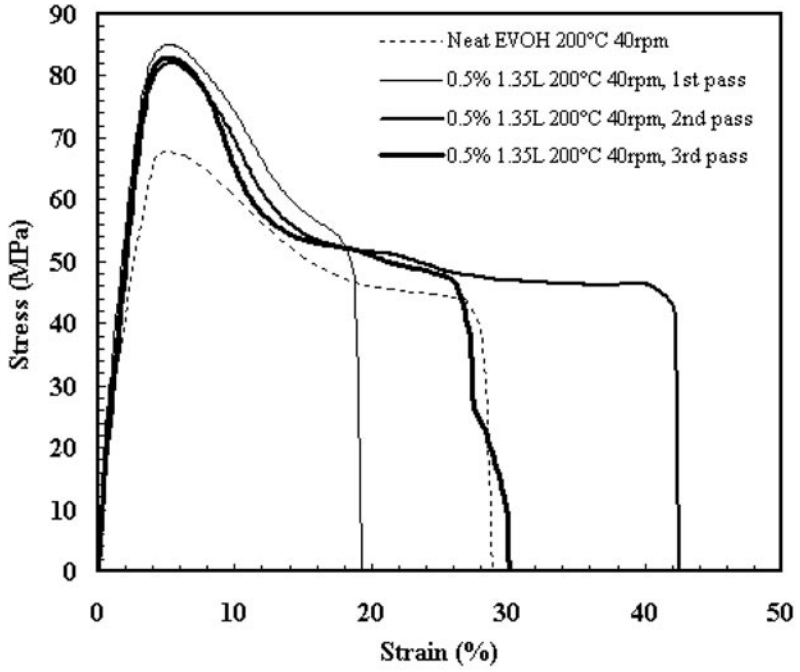

Fig. 5. Stress-strain curves of EVOH containing 0.5 wt% I.35L clay after three successive passes in the extruder at 200°C and 40 rpm and injection molding.

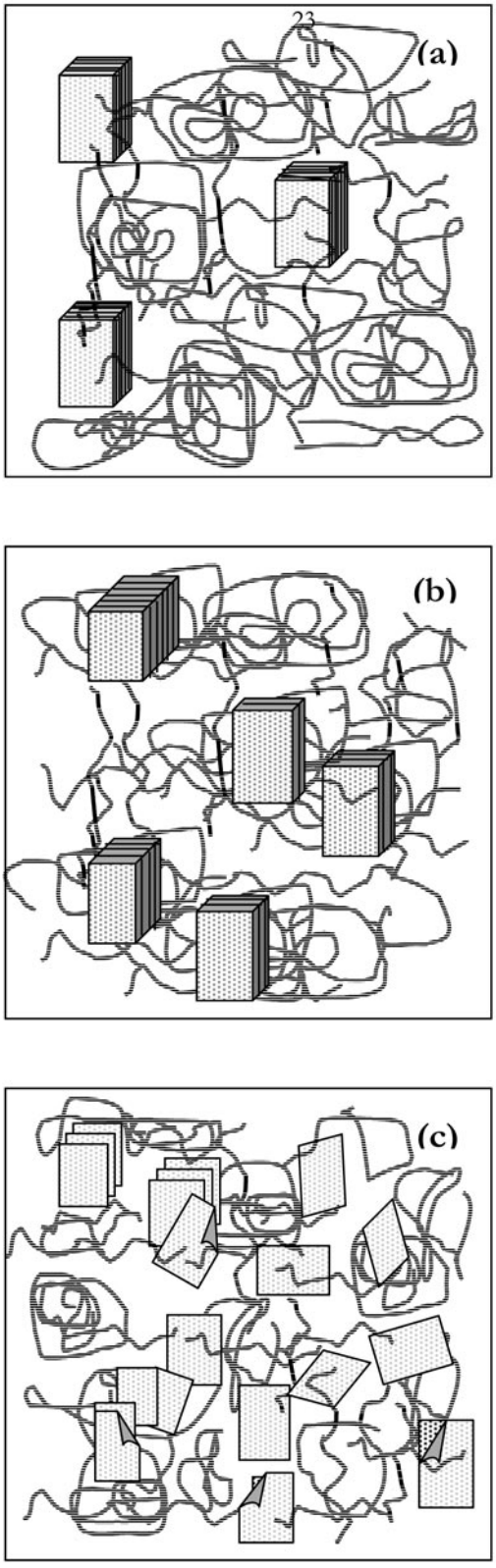

Fig. 6. Schematic description of clay fracturing and an onion-like delamination process, where thin platelets peel off and blend into the matrix: (a) before intercalation and/or delamination process, (b) intercalation and clay fracturing, (c) advanced delamination process.

(2θ = 2.72°). Reference samples of 85/15 EVA-g-MA/clay and 85/15 LLDPE-g-MA/clay were examined to characterize the tendency of each compatibilizer by itself to intercalate, showing significantly different gallery heights of 42 and 29Å, respectively. The EVOH/clay systems containing 1, 5 and 10 wt% EVA-g-MA exhibit characteristic peaks at 2.6, 2.5 and 2.3° (d_{001} = 33, 35 and 38Å), respectively. The gallery heights of the corresponding blends containing LLDPE-g-MA (not shown here) are 34, 35 and 38Å, respectively, same as obtained for the EVA-g-MA. Although EVA-g-MA itself tends to intercalate more than LLDPE-g-MA and more than EVOH, the final gallery heights were similar for the two compatibilizers. When EVA-g-MA is added, there may be a competition between the compatibilizer and the EVOH regarding the intercalation process. Therefore, in this case, probably EVA-g-MA is also intercalated and more EVOH remains outside the galleries compared to the content of EVOH outside when LLDPE-g-MA is used.

The thermal behavior of EVOH is strongly affected by the presence of the clay and processing conditions (see *Table 1*). Polymer chains attached to the platelets are partially hindered from taking part in the flow process, and their crystallization process is also hindered. Thus, the platelets affecting the crystallization process are both those in the intercalated particles and those already dispersed. EVOH containing 15 wt% I.30E clay that was melt-mixed in a Brabender Plastograph for 10 min shows a T_m of 178.9°C, similar to the neat EVOH (179.6°C), but a lower enthalpy value, 72.2 mJ/g (normalized to EVOH content), compared to 82.7 mJ/g for the neat EVOH. After 45 min of mixing, much lower melting temperature and enthalpy values, 159.5°C and 55.5 mJ/g respectively, are found. These results differ from reports on other systems (9, 19, 20). The crystallization process in the presence of clay particles, especially clay nano-platelets, generates smaller EVOH crystals, having a lower melting temperature. Probably, the clay plays a role of a "low-quality nucleating agent," which in addition hinders the crystallization process, owing to its high interaction level with EVOH.

Significant changes in the EVOH melting behavior are observed when compatibilizers are added (*Table 1*), which are more significant for higher amounts of compatibilizer. The thermal characteristics of EVOH containing different amounts of EVA-g-MA, without clay, are similar to those of the neat EVOH (not shown here). When clay is incorporated, the melting temperatures (T_m) of 84/15/1 and 80/15/5 EVOH/clay/EVA-g-MA (166°C and 160°C, respectively) are higher compared to that of the uncompatibilized 85/15 EVOH/clay blend (156°C). However, the reduction of the melting temperature compared to the neat EVOH (180°C) is significant. Interestingly, at 10 wt% EVA-g-MA, no melting peak is observed, indicating the absence of crystalline phase in this case. The reduced crystallinity, as presented by the heat of fusion, is also higher for the blends containing 1 and 5 wt% compatibilizer compared to the uncompatibilized blend (41, 34 and 32 m W/g, respectively).

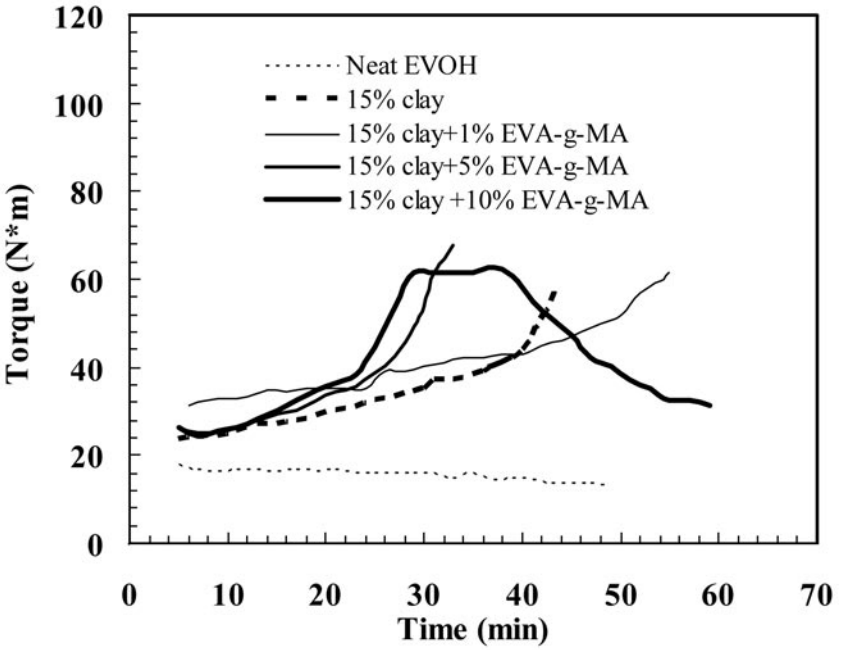

Fig. 7. Brabender plastograms of EVOH/I.30E clay systems containing EVA-g-MA, at 230°C and 60 rpm.

Similar trends were observed for the crystallization process. The 84/15/1 EVOH/clay/LLDPE-g-MA blend showed less interruption to the EVOH crystallization process; however, when 5 wt% LLDPE-g-MA was used, the interruption was significant, and for 10 wt% LLDPE-g-MA, no crystallization occurred. This stems from the high interaction levels developed between the EVOH and the clay in the presence of the compatibilizers; thus, ultimately, EVOH segments cannot crystallize. Moreover, the intercalation level increases for higher compatibilizer contents; therefore, more delamination and exfoliation occur, resulting in more dispersion of single platelets, which further reduces crystallization.

When only 1 wt% of clay was incorporated, although an exfoliated structure was obtained (after extrusion and injection molding), no interruption to the EVOH crystallization process was obtained. Thus, EVOH thermal behavior is greatly affected by the clay content and processing conditions. Competition results between the clay reinforcing effect and the deterioration of

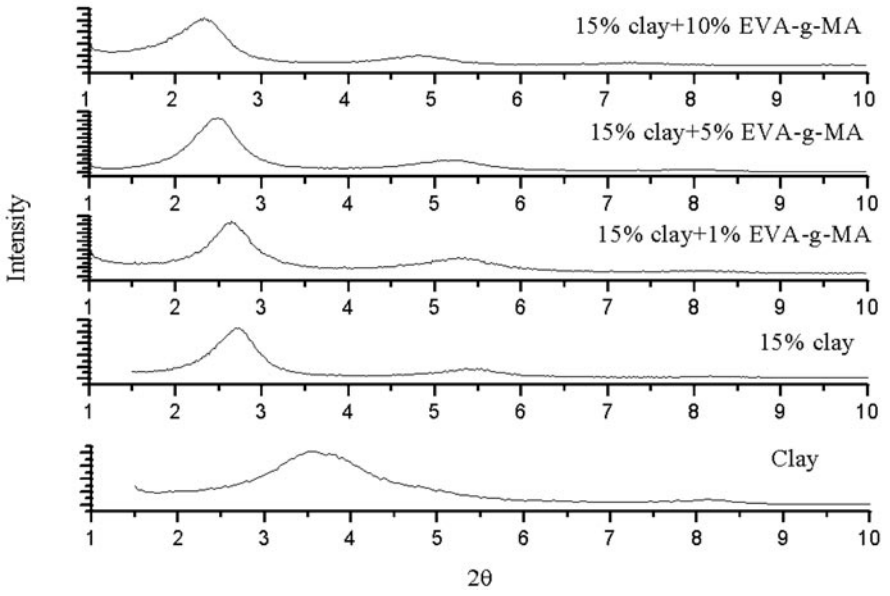

Fig. 8. X-ray diffraction patterns of EVOH/I.30E clay systems containing EVA-g-MA.

Table 1. Thermal Characteristics of EVOH/Clay/Compatibilizer Nanocomposite Systems Containing EVOH and 15 wt% Clay.

	T_c (°C)	ΔHc (mW/g)	T_m (°C)	ΔHm (mW/g)
EVOH	160	60	180	82
EVOH + 15% clay	341	29	156	32
*1% EVA-g-MA	158	35	166	41
*5% EVA-g-MA	132	30	159	34
*10% EVA-g-MA	—	0	—	0
*1% LLDPE-g-MA	157	30	162	35
*5% LLDPE-g-MA	98	15	135	20
*10% LLDPE-g-MA	—	0	—	0

*Containing EVOH + 15% clay.

mechanical properties, owing to a dramatic drop in crystallinity. Therefore, optimal processing conditions must be sought in order to achieve improved properties.

CONCLUSIONS

- EVOH is a unique matrix polymer for nanocomposites because of the strong interactions it develops with the clay particles.
- Dynamic melt-mixing of EVOH/treated organo-clay mixtures is accompanied by a significant torque increase owing to clay particle fracturing, intercalation and delamination processes and the buildup of significant levels of polymer/clay interaction.
- The dominant step in dynamic melt blending is delamination (exfoliation) of clay particles, according to the onion-like delamination model suggested.
- Mixed morphology of intercalation and delamination or complete exfoliation can be achieved, depending on blending conditions and clay content.
- The addition of compatibilizers enhances the intercalation levels of EVOH into clay galleries.
- Compatibilizers by themselves intercalate into clay galleries.
- The thermal behavior of EVOH in the EVOH/clay systems is greatly affected by the presence of the clay. The melting temperature and crystallinity level dramatically decrease.
- T_m, T_c and the degree of crystallinity of the EVOH in the presence of clay decrease with increasing compatibilizer content, until at a certain content no crystallization takes place, owing to high intercalation level of the EVOH, exfoliation of the clay, and interactions between EVOH and clay in the presence of the compatibilizer.

ACKNOWLEDGMENT

The authors are grateful to the Israel Ministry of Science for partially supporting the nanocomposite project. N. Artzi acknowledges the generous Levi Eshkol scholarship from the Israel Ministry of Science.

REFERENCES

1. R. A. Vaia, H. Ishii, and E. P. Giannelis, *Chem. Mater.*, **5**, 1694 (1993).
2. K. Masenelli-Varlot, E. Reynaud, G. Vigier, and J. Varlet, *J. Polym. Sci., Part B: Polym. Phys.*, **40**, 272 (2002).
3. J. W. Cho and D. R. Paul, *Polymer*, **42**, 1083 (2001).
4. R. A. Vaia, B. B. Sauer, O. K. Tse, and E. P. Giannelis, *J. Polym. Sci., Part B: Polym. Phys.*, **35**, 59 (1997).
5. N. Hasegawa, M. Kawasumi, M. Kato, Usuki, and A. Okada, *J. Appl. Polym. Sci.*, **67**, 87 (1998).
6. R. A. Vaia, K. D. Jandt, E. J. Kramer, and E. P. Giannelis, *Chem. Mater.*, **8**, 2628 (1996).
7. P. Reichert, J. Kressler, R. Thomann, R. Mulhaupt, and G. Stoppelmann, *Acta Polymer*, **49**, 116 (1998).
8. P. B. Messersmith and E. P. Giannelis, *J. Polym. Sci., Part A: Polym. Chem.*, **33**, 1047 (1995).
9. R. A. Vaia, S. Vasudevan, W. Krawiec, L. G. Scanlon, and E. P. Giannelis, *Adv. Mater.*, **7**, 154 (1995).
10. A. Usuki, M. Kato, A. Okada, and T. Kurauchi, *J. Appl. Polym. Sci.*, **63**, 137 (1997).
11. Y. Kurokawa, H. Yashuda, and A. Oya, *J. Mater. Sci., Lett.*, **15**, 1481 (1996).
12. A. Okada and A. Usuki, *Mater. Sci. Eng.*, **C3**, 109 (1995).
13. C. Zilg, R. Thomann, R. Mulhaupt, and J. Finter, *Adv. Mater.*, **1**, 49 (1999).
14. N. Hasegawa, H. Okamoto, M. Kawasumi, and A. Usuki, *J. Appl. Polym. Sci.*, **74**, 3359 (1999).
15. X. Kornmann, H. Lindberg, and L. A. Berlund, *SPE ANTEC '99*, 1623 (1999).
16. S. Wang, C. Long, X. Wang, Q. Li, and Z. Qi, *J. Appl. Polym. Sci.*, **69**, 1557 (1998).
17. N. Artzi, Y. Nir, D. Wang, M. Narkis, and A. Siegmann, *Polym. Compos.*, **22**, 710 (2001).
18. N. Artzi, Y. Nir, M. Narkis, and A. Siegmann, *J. Polym. Sci., Part B: Polym. Phys.*, **40**, 1741 (2002).
19. E. P. Giannelis, *Adv. Mater.*, **8**, 29 (1996).
20. L. Liu, Z. Qi, and X. Zhu, *J. Appl. Polym. Sci.*, **71**, 1133 (1999).
21. X. Kornmann, L. A. Berglund, J. Sterte, and E. P. Giannelis, *Polym. Eng. Sci.*, **38**, 1351 (1998).
22. N. Nemirovski and M. Narkis, *Makromol. Chem., Macromol. Symp.*, **76**, 241 (1993).
23. N. Artzi, Y. Nir, M. Narkis, and A. Siegmann, *Polym. Compos.*, **24**, 627 (2003).